Available online at www.sciencedirect.com

ScienceDirect

Mendeleev Commun., 2022, **32**, 371–373

Mendeleev Communications

New D–A–D luminophores of the [1,2,5]thiadiazolo[3,4-*d*]pyridazine series

Vladislav M. Korshunov,*[a] Timofey N. Chmovzh,[b,c] German R. Chkhetiani,[b] Ilya V. Taydakov[a] and Oleg A. Rakitin*[b]

[a] *P. N. Lebedev Physical Institute, Russian Academy of Sciences, 119991 Moscow, Russian Federation. E-mail: vladkorshunov@bk.ru*

[b] *N. D. Zelinsky Institute of Organic Chemistry, Russian Academy of Sciences, 119991 Moscow, Russian Federation. E-mail: orakitin@ioc.ac.ru*

[c] *Nanotechnology Education and Research Center, South Ural State University, 454080 Chelyabinsk, Russian Federation*

DOI: 10.1016/j.mencom.2022.05.026

Three [1,2,5]thiadiazolo[3,4-*d*]pyridazines containing 4,7-positioned indole-type substituents were synthesized from the corresponding 4,7-dibromo precursor employing the S_NAr aromatic nucleophilic substitution. Photophysical properties and DFT calculations showed that the D–A–D dyes based on [1,2,5]thiadiazolo[3,4-*d*]pyridazine core exhibited fluorescence in the near infrared region of the spectrum, which makes them promising for use as an active emitting layer in NIR-OLEDs as well as for other possible applications as an IR luminophore.

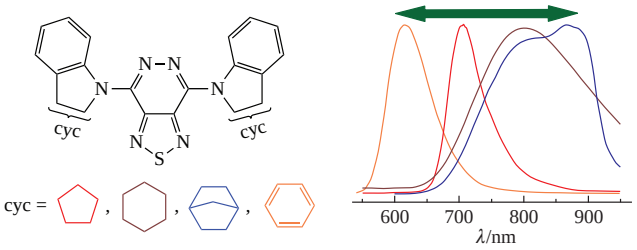

Keywords: [1,2,5]thiadiazolo[3,4-*d*]pyridazines, indoles, aromatic nucleophilic substitution, luminescence, donor–acceptor–donor structure, synthesis, NIR-OLEDs.

Small organic molecules based on fused 1,2,5-thiadiazoles containing donor (D) and acceptor (A) building blocks are widely used to design various electronic devices such as dye sensitized solar cells (DSSCs),[1] bulk heterojunction solar cells,[2] n-type organic field-effect transistors,[3] materials capable of luminescence in the entire visible range of the spectrum as well as in the near infrared part of the spectrum.[4] Special attention is paid to structures of the donor–acceptor–donor (D–A–D) type since the introduction of an additional donor improves the properties of the intramolecular charge transfer (ICT) mechanism.[5] Interest in dyes of this family is primarily associated with the ability to widely vary donor and acceptor molecular fragments, achieving the necessary characteristics of the target products by fine tuning the energy difference between the highest occupied molecular orbital (HOMO) and the lowest unoccupied molecular orbital (LUMO), and, consequently, the positions absorption and luminescence maxima. Although various acceptors based on fused derivatives of 1,2,5-thiadiazole such as benzo[*d*][1,2,3]thiadiazole[6] or benzo[1,2-*d*:4,5-*d*′]bis([1,2,3]-thiadiazole)[7] are known, there is a need to search for new acceptor groups from heterocyclic systems based on 1,2,5-thiadiazole to create new highly efficient luminescent materials with improved special properties.

Recently, quantum chemical calculations revealed that the [1,2,5]thiadiazolo[3,4-*d*]pyridazine fragment has not only the lowest HOMO energy but also the highest electron-withdrawing properties, which should lead to a decrease in the energy gap in D–A–D structures.[8] Indeed, it was shown that the introduction of [1,2,5]thiadiazolo[3,4-*d*]pyridazine as a molecular fragment with pronounced electronic acceptor properties into a conjugated polymer consisting of thienyl donor substituents leads to a decrease in the energy gap to 1.5 eV and to a shift of the absorption spectrum to longer wavelengths in comparison with analogous compounds based on pyridothiadiazoles.[3(b)] However, until now, there have been no data on the luminescence characteristics of compounds based on [1,2,5]thiadiazolo[3,4-*d*]-pyridazine.

In this work, new compounds of the D–A–D type based on [1,2,5]thiadiazolo[3,4-*d*]pyridazine acting as an acceptor, as well as 1,2,3,3a,4,8b-hexahydrocyclohexa[*b*]indole, 1,2,3,3a,4,8b-hexahydrocyclopenta[*b*]indole, 1,2,3,4,4a,9a-hexahydro-9λ^2-1,4-methanocarbazole, and carbazole acting as donor fragments were obtained and investigated. The effect of the structure of these molecular blocks on the luminescence characteristics of the obtained dyes was established.

We have previously investigated the behavior of 4,7-dibromo[1,2,5]thiadiazolo[3,4-*d*]pyridazine **1** in nucleophilic aromatic substitution (S_NAr) reactions with a number of amines and found the optimal conditions for the synthesis of disubstituted derivatives [1,2,5]thiadiazolo[3,4-*d*]pyridazines of type **2** (Scheme 1).[9] Carrying out the reaction of dibromide **1** with two equivalents of amine **3** in the presence of two equivalents of triethylamine while refluxing the reaction mixture in MeCN for 3 h afforded the target products **2** most smoothly. We employed the optimized conditions for nucleophilic substitution reactions of 1,2,3,3a,4,8b-hexahydrocyclopenta[*b*]indole **3a**, 1,2,3,3a,4,8b-hexahydrocyclohexa[*b*]indole **3b** and 1,2,3,4,4a,9a-hexahydro-9λ^2-1,4-methanocarbazole **3c** and obtained bis-substitution products **2a**–**c** in high yields.

However, it was not possible to obtain another candidate for high-performance luminescent compounds, namely, 4,7-di(9*H*-carbazol-9-yl)benzo[*c*][1,2,5]thiadiazole **4**, because dibromo derivative **1** did not react with carbazole either under aromatic nucleophilic substitution conditions as well as under Buchwald–

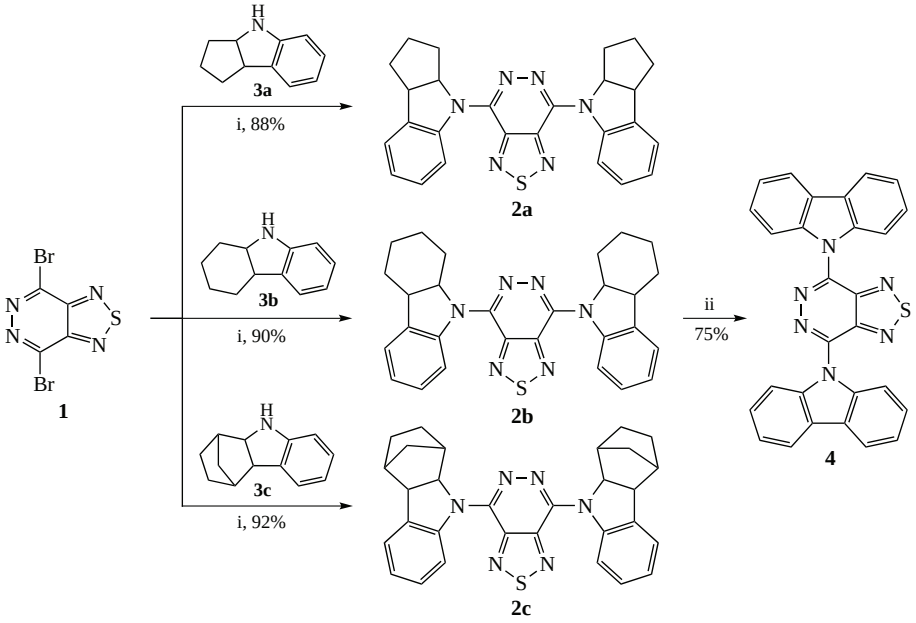

Scheme 1 *Reagents and conditions*: i, Et_3N, MeCN, 80 °C, 10–30 h; ii, DDQ, PhMe, Δ, 7 h.

Hartwig or Ullmann conditions due to the low nucleophilicity of carbazole.[8(a)] Meanwhile, a D–A–D-type compound **4** with two carbazole moieties was successfully synthesized from bis(hexahydrocarbazolyl) derivative **2b** by its treatment with DDQ (see Scheme 1).[9] The structures of the target compounds D–A–D were unambiguously confirmed by elemental analysis, IR, ^{1}H and ^{13}C NMR spectroscopy, high-resolution mass spectrometry and mass spectrometry (see Online Supplementary Materials).

Optical absorption spectra were measured for all studied compounds **3a**–**c** and **4** in solvents with different polarities. The spectra consist of several spectral bands in the UV range of wavelengths and one broad band in the visible range of the spectrum, which is explained by the ICT process. For compound **4**, the maximum of the ICT band is located in the spectral region of 479–526 nm, depending on the polarity of the solvent, while the other substances exhibit absorption in the orange-red region. The main photophysical parameters such as absorption maximum wavelength λ_{abs}, maximum molar extinction ε_{max}, emission maximum wavelength λ_{em}, and Stokes shift $\Delta\nu$ are given in Table 1. It was found that with increasing solvent polarity, a noticeable blue shift of the long-wavelength (ICT) band in the absorption spectra occurs. In this case, the maximum shift of ICT absorption wavelength by 30–40 nm from the positions obtained for the solution in chloroform is observed for solutions in acetonitrile (see Online Supplementary Materials, Figure S1 and Table S1).

The spectra obtained for **2a**–**c** in the UV region are qualitatively similar and have an absorption maximum at a wavelength of 295–300 nm. The position of this short-wavelength maximum does not depend on the polarity of the solvent and is the same for compounds **2a**–**c**, which indicates that this band is associated with the π–π* electronic transfer, and the orbitals involved in the transfer are delocalized throughout the molecule. The introdution of the donor 9*H*-carbazol-9-yl fragment in compound **4** resulted in the π–π* transition band undergoing a hypsochromic shift up to 275 nm (see Table S1).

The investigated substances **2a**–**c** exhibit bright fluorescence in the near infrared (NIR) range of the spectrum (λ_{max} = 700–900 nm), while compound **4** emits mainly in the visible region of the spectrum (see Table S1 and Figure 1). The luminescence maximum of substance **2b** shifts to the NIR region (λ_{max} = 794–820 nm) with an increase in the polarity of the solvent. Thus, this substance can be used as an emitting layer in NIR-OLED and other possible applications as an NIR luminophore. On the contrary, for other substances the wavelength of the maximum radiation has a more complex dependence on the polarity of the medium. We observe a red shift of the emission maximum with increasing polarity; however, in the polar solvent MeCN (Δf = 0.305), the emission maximum unexpectedly shifts towards shorter wavelengths by 151 nm for compound **2a** and by 80 nm for compound **4**. To clarify the dependence of the emission maximum on the polarity of the medium, additionally, the luminescence spectra of compound **4** in DMF and acetone were obtained. It was found that the wavelength of the maximum radiation is the same for both solutions and slightly differs in comparison with solutions with maxima for THF and DMSO (see Figure S3). Thus, the blue shift of the luminescence band is a specific property for solutions of these compounds in acetonitrile.

In order to gain insight into electronic transitions observed in the spectra, we performed quantum chemical calculations using the DFT and TD-DFT methods at the wB97XD/cc-pVDZ level of theory. The estimated wavelengths of low-energy absorption

Table 1 Experimental and calculated values of the main photophysical parameters of the investigated substances (in $CHCl_3$).

Dye	λ_{abs}/ nm	ε_{max}/ ×10^4	λ_{em}/ nm	Stokes shift/cm^{-1}	S_0–S_1[a]/ nm	f[a]	Major contribution[a]
2a	580	3.1	706	3062	479.8	0.36	HOMO→LUMO (95%)
2b	568	1.0	802	5137	482.2	0.35	HOMO→LUMO (96%)
2c	595	6.1	751	3720	499.4	0.33	HOMO→LUMO (95%)
4	525	2.2	695	4623	434.6	0.28	HOMO→LUMO (90%)

[a] Calculated values.

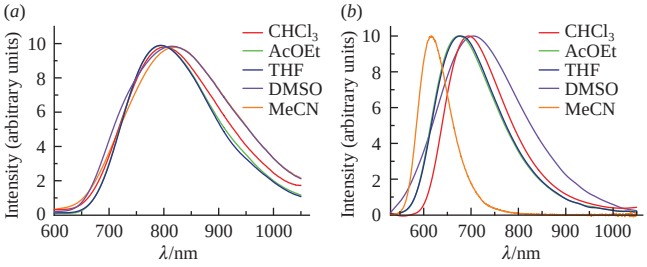

Figure 1 Luminescence spectra recorded for (*a*) dye **2b** and (*b*) dye **4**.

band and corresponding oscillator strengths are listed in Table 1. The calculated absorption wavelengths are higher than experimental ones but have the same trend. The oscillator strength amplitudes are approximately the same (f = 0.28–0.36) suggesting that altering of donor unit does not significantly increase optical absorption. From the analysis of contributions of single interactions and the frontier molecular orbitals obtained for the dyes we conclude that long-wavelength absorption bands can be assigned to intramolecular charge transfer process. The transfer between the molecular orbitals HOMO and LUMO has the largest contribution (90–95%) to the S_0–S_1 energy transfer. According to Figure S4 (see Online Supplementary Materials), HOMO is localized predominantly on the phenyl rings of the donor fragments and on the pyridazine of the central acceptor, opposite LUMO is localized on the acceptor block and nitrogen atoms of the donor fragments. This result confirms that the long-wavelength absorption band in the spectra is of the nature of intramolecular charge transfer to the thiadiazolopyridazine fragment.

In conclusion, new dyes based on [1,2,5]thiadiazolo[3,4-*d*]-pyridazine exhibiting bright fluorescence in the near infrared region of the spectrum were obtained. The introduction of aromatic (carbazole) donor fragments into this molecule leads to a spectral shift of the luminescence to the visible region of the spectrum, and for dyes with two indoline donor fragments the luminescence maximum is shifted to the NIR region (λ_{max} = 794–820 nm). In addition, several dyes were found to exhibit unusual behavior of the luminescence maximum in a polar medium. So, the use of acetonitrile as a solvent leads to a change in the emission wavelength in the blue region of the spectrum from 80–150 nm in comparison with less polar solvents. Thus, D–A–D dyes based on thiadiazolopyridazine were shown to exhibit fluorescence in the near infrared region of the spectrum, which makes them a promising class of materials for use as an active emitting layer in NIR-OLED, as well as for other possible applications as an NIR phosphor.

We gratefully acknowledge financial support from the Russian Science Foundation (grant no. 20-73-00220).

Online Supplementary Materials

Supplementary data associated with this article can be found in the online version at doi: 10.1016/j.mencom.2022.05.026.

References

1 (*a*) E. A. Knyazeva and O. A. Rakitin, *Russ. Chem. Rev.*, 2016, **85**, 1146; (*b*) E. A. Knyazeva, W. Wu, T. N. Chmovzh, N. Robertson, J. D. Woollins and O. A. Rakitin, *Sol. Energy*, 2017, **144**, 134; (*c*) B. A. D. Neto, A. A. M. Lapis, E. N. da Silva, Jr., and J. Dupont, *Eur. J. Org. Chem.*, 2013, 228; (*d*) M. Yahya, A. Bouziani, C. Ocak, Z. Seferoğlu and M. Sillanpää, *Dyes Pigm.*, 2021, **192**, 109227; (*e*) S. Chaurasia and J. T. Lin, *Chem. Rec*., 2016, **16**, 1311.

2 (*a*) A. V. Akkuratov and P. A. Troshin, *Polym. Sci., Ser. B*, 2014, **56**, 414 (*Vysokomol. Soedin., Ser. B*, 2014, **56**, 371); (*b*) G. V. Bulavko and A. A. Ishchenko, *Russ. Chem. Rev.*, 2014, **83**, 575; (*c*) T. P. Le, B. H. Smith, Y. Lee, J. H. Litofsky, M. P. Aplan, B. Kuei, C. Zhu, C. Wang, A. Hexemer and E. D. Gomez, *Macromolecules*, 2020, **53**, 1967; (*d*) W. Xu, Y. Chang, X. Zhu, Z. Wei, X. Zhang, X. Sun, K. Lu and Z. Wei, *Chin. Chem. Lett*., 2022, **33**, 123; (*e*) A. Wadsworth, Z. Hamid, J. Kosco, N. Gasparini and I. McCulloch, *Adv. Mater*., 2020, **32**, 2001763.

3 (*a*) R. Zhao, Y. Min, C. Dou, B. Lin, W. Ma, J. Liu and L. Wang, *ACS Appl. Polym. Mater*., 2020, **2**, 19; (*b*) A. Leventis, T. N. Chmovzh, E. A. Knyazeva, Y. Han, M. Heeney, O. A. Rakitin and H. Bronstein, *Polym. Chem.*, 2020, **11**, 581; (*c*) Z. Tang, X. Wei, W. Zhang, Y. Zhou, C. Wei, J. Huang, Z. Chen, L. Wang and G. Yu, *Polymer*, 2019, **180**, 121712.

4 (*a*) A. C. Stuart, J. R. Tumbleston, H. Zhou, W. Li, S. Liu, H. Ade and W. You, *J. Am. Chem. Soc.*, 2013, **135**, 1806; (*b*) V. M. Korshunov, T. N. Chmovzh, E. A. Knyazeva, I. V. Taydakov, L. V. Mikhalchenko, E. A. Varaksina, R. S. Saifutyarov, I. C. Avetissov and O. A. Rakitin, *Chem. Commun*., 2019, **55**, 13354; (*c*) V. M. Korshunov, T. N. Chmovzh, I. S. Golovanov, E. A. Knyazeva, L. V. Mikhalchenko, R. S. Saifutyarov, I. C. Avetisov, J. D. Woollins, I. V. Taydakov and O. A. Rakitin, *Dyes Pigm*., 2021, **185**, 108917.

5 (*a*) S. Biswas, *Chem. Phys. Lett*., 2016, **649**, 23; (*b*) P. Chen, H. Zhu, L. Kong, X. Xu, Y. Tian and J. Yang, *Dyes Pigm.*, 2020, **172**, 107832.

6 (*a*) P. S. Gribanov, D. A. Lypenko, A. V. Dmitriev, S. I. Pozin, M. A. Topchiy, A. F. Asachenko, D. A. Loginov and S. N. Osipov, *Mendeleev Commun*., 2021, **31**, 33; (*b*) O. A. Rakitin, *Tetrahedron Lett*., 2020, **61**, 152230.

7 (*a*) A. Minotto, P. Murto, Z. Genene, A. Zampetti, G. Carnicella, W. Mammo, M. R. Andersson, E. G. Wang and F. Cacialli, *Adv. Mater.*, 2018, **30**, 1706584; (*b*) L. Bianchi, X. Zhang, Z. Chen, P. Chen, X. Zhou, Y. Tang, B. Liu, X. Guo and A. Facchetti, *Chem. Mater*., 2019, **31**, 6519.

8 (*a*) T. N. Chmovzh, E. A. Knyazeva, L. V. Mikhalchenko, I. S. Golovanov, S. A. Amelichev and O. A. Rakitin, *Eur. J. Org. Chem*., 2018, **41**, 5668; (*b*) T. N. Chmovzh, E. A. Knyazeva, N. V. Krukovskaya and O. A. Rakitin, *Russ. Chem. Bull*., 2020, **69**, 2167.

9 T. N. Chmovzh, E. A. Knyazeva, K. A. Lyssenko, V. V. Popov and O. A. Rakitin, *Molecules*, 2018, **23**, 2576.

Received: 6th October 2021; Com. 21/6718